Proceedings of ASME Turbo Expo 2012
GT2012
June 11-15, 2012, Copenhagen, Denmark

GT2012-69456

A PATH TOWARDS THE AERODYNAMIC ROBUST DESIGN OF LOW PRESSURE TURBINES

Francesco Bertini
Martina Credi
Avio S.p.A.
via I Maggio, 99
10040, Rivalta di Torino (TO), Italy
francesco.bertini@aviogroup.com

Michele Marconcini
Matteo Giovannini
"Sergio Stecco" Department of Energy Engineering
University of Florence
via di Santa Marta, 3, 50139 Firenze, Italy
michele.marconcini@unifi.it

ABSTRACT

Airline companies are continuously demanding lower-fuel-consuming engines and this leads to investigating innovative configurations and to further improving single module performance. In this framework the Low Pressure Turbine (LPT) is known to be a key component since it has a major effect on specific fuel consumption (SFC).

Modern aerodynamic design of LPTs for civil aircraft engines has reached high levels of quality, but new engine data, after first engine tests, often cannot achieve the expected performance. Further work on the modules is usually required, with additional costs and time spent to reach the quality level needed to enter in service. The reported study is aimed at understanding some of the causes for this deficit and how to solve some of the highlighted problems.

In a real engine, the LPT module works under conditions which differ from those described in the analyzed numerical model: the definition of the geometry cannot be so accurate, a priori unknown values for boundary conditions data are often assumed, complex physical phenomena are seldom taken into account, operating cycle may differ from the design intent due to a non-optimal coupling with other engine components. Moreover, variations are present among different engines of the same family, manufacturing defects increase the uncertainty and, finally, deterioration of the components occurs during service.

Research projects and several studies carried out by the authors lead to the conclusion that being able to design a module whose performance is less sensitive to variations (Robust LPT) brings advantages not only when the engine performs under strong off-design conditions but also, due to the abovementioned unknowns, near the design point as well.

Concept and Preliminary Design phases are herein considered, highlighting the results arising from sensibility studies and their impact on the final designed robust configuration. Module performance is afterward estimated using a statistical approach.

INTRODUCTION

Current tendencies in commercial aero-engines, as required to satisfy ACARE [1] goals, lead to increase BPR, in order to significantly reduce SFC and noise emissions. As a consequence, LPT modules operate under critical conditions due to the greater work requested.

Furthermore, solutions adopted for recent aero-engines push towards a reduction in stage number (HSL) and airfoil count for each row (HL): the former having an important impact on weight and axial dimensions, the latter on part count, and both with a major positive effect on costs. To produce the amount of work requested, LPT blades have then to work with high loading factor values requiring higher flow-deflections. These conditions limit LPT robustness, intended as the capability to maintain module performance when operating conditions move away from design intent.

Despite the improvements in the design process and in the numerical tools, greater critical operating conditions for the LPT modules do not allow for a reduction in the discrepancies between the predictions and the measured engine performance. The main cause of this mismatch could be linked to the fact that, generally, a LPT real module operates under different conditions from those supposed in the design phase. According to engine data, innovative configurations seem to be more sensitive to differences between modeling and real engine conditions.

Such differences are reported in the available literature: in [2], the authors show that, from a robust sensitivity assessment performed on strut and frame of a prediffuser, main noise factors are manufacturing uncertainties and custom usage. In [3], manufacturing uncertainties in a compressor blade are reported, while, in [4], problems of erosion in a compressor fan are studied. Uncertainties impact on the thermodynamic cycle in a gas turbine compressor system is taken into account in [5]. Specific analyses on the causes that lead the reality to differ from the studied models are found in [6–8] for gas turbines. However, no paper examines the causes of such discrepancies in a comprehensive way.

Theoretical models differ from the experimental turbine engine even when operating conditions are coincident. This means that real modules would generally perform worse than design intent even at design point conditions. The present work stems from the authors' belief that a LPT module optimized to maintain high levels of performance even in off-design conditions is expected to present a lower deficit in

efficiency when tested, due to positive implications of robust design not only in off-design conditions but also at design point, a topic which is not specifically highlighted in the past literature.

Papers usually focus on the importance of multidisciplinary robust design in different fields and suggest several methodologies to approach the problem: games theory in sequential Stackelberg leader/follower model in [9], various Six Sigma approaches (QFD matrix, P-diagram, what-why table) in [2], essential stages of robust design optimization using a mathematical point of view in [10] and a multidisciplinary robust approach for turbo-machinery in [11]. Available papers basically include a statistical approach to find a robust configuration but, in order to simplify the complex mathematical problem, they only include analyses on a specific source of uncertainties, drastically simplifying the problem, and using low-fidelity surrogate models instead of detailed CFD-CAE tools to reduce computational costs.

Only a few papers deal with aeronautical turbines' robustness and even less are specifically devoted to LPT modules. Some of these works concern structural aspects and mainly there is no literature at all dedicated to them from an aerodynamic point of view.

There are two different methodological approaches to solve the problem of finding a robust designed configuration. The one generally followed and described mainly in all papers deals with a stochastic analysis of uncertainties effects. This is the case of Taguchi methods [3, 4, 7, 9], Bayesian Monte Carlo simulation [3] or polynomial chaos [5].

The methodology adopted in the present work is quite different. We started analyzing the discrepancies between real engines and numerical models, then, main impacts of these features on numerical aerodynamic analyses were identified in a form easily simulated with standard CFD codes and a solution, robust to these deviations, was deterministically found. Only at the end of this optimization process, a statistical approach was used to verify that the configuration obtained was really robust, and to estimate the benefit under design point conditions.

An advantage of the proposed methodology is that it allows one to take all the main unknown effects into account, and then to extrapolate effective robust design criteria and golden rules, in order to replicate the results on future LPT designs.

DIFFERENCES BETWEEN DESIGN MODELS AND REALITY

The main differences between models and real engines are described below:

Geometrical differences. Structural and fluid dynamic analyses are typically performed with simplified models that do not exactly reproduce the real turbine geometry. In fact, especially during design phases, the models adopted generally neglect the presence of some geometrical details, like steps or gaps between adjacent rows, fillets at endwalls, rotor tip clearances, secondary air system cavities, and leakages. All these approximations, which ignore some important phenomena, cast uncertainties on the obtained results.

Modeling limitations. From a physical point of view there are two main issues. On the one hand, there are intrinsic limits in the mathematical methods used to solve Navier-Stokes equations. This includes all differences due to the mathematical approximation of a real phenomenon. Currently, most of the CFD analyses are typically performed in steady conditions, thus neglecting the effects of wakes and interactions among rows. Using discrete formulation and turbulence models for Navier-Stokes equations, although correctly approximating flow behavior, obviously represents another error source; ideal gas behavior is likewise usually supposed. Furthermore, aero-elastic and thermo-mechanic effects could be non-negligible in terms of local variations to flow field, as both tend to slightly change component shapes and geometries, but generally their effects are not included in CFD analyses.

On the other hand, there are limitations due to uncertainties on boundary conditions. The LPT module, due to a non-optimal coupling with all the other engine parts, could easily work in conditions quite different from the original intent and, in addition, the way the engine is installed on the aircraft and its interaction with fuselage and wings can significantly affect the operating conditions.

For example, during the design phase, upstream flow can only be estimated, generally using simplified distributions circumferentially averaged. Consequently, TCF wakes are completely ignored, although they are experimentally found even after the first 3-4 downstream LPT stages. Uncertainties on some parameters used by numerical models, like inlet turbulence levels, length scale or roughness also have to be taken into account.

Theoretically almost all of these effects could be inserted into a complete CFD analysis. Many papers address detailed CFD simulations considering the impact of some of these sources of uncertainty, but in a traditional design process they are usually neglected, both for strict time schedules and for intrinsic lack of information. A detailed report on limitations of turbomachinery CFD is contained in [12].

Engine-to-Engine variation. Variations are present between different engines of the same family. Once an aircraft is put on the market, its production period is usually quite long and during this time the numerous components can undergo changes and updating. Some parts can be modified for technical reasons or considerations on production cost optimization, and this could have a non-negligible impact on the operative cycle. Airline companies can also require specific design modifications on some engine components, according to particular requirements or needs.

Manufacturing defects. During the design phase the geometries are defined to respect specific tolerance ranges usually determined as having a small impact on FF and traditionally analyzed overall module performance. Local effects of these variations on the flow field are instead not taken into account.

In-service deterioration. Strong deterioration events affect the turbine during its long operative life cycle. These are much more considerable on the HPT, which is immediately downstream of the combustor and directly subjected to hot streams; anyway some effects are also evident on the low pressure turbine stages. In-service deterioration causes modifications of original geometries, e.g. an increase in surface roughness (its effects are visible even after a few operational hours), trailing edge erosion with local alteration of outlet flow angle, fins rubbing the honeycomb. Due to the reduced performance of the various components, to guarantee the same thrust, SFC must be augmented, thus increasing inlet temperature for LPT and reducing corrected speed ($N/\sqrt{T_0}$) with major effects on airfoil incidence.

Due to the complexity of the described phenomena, it is almost impossible to correctly simulate all the variations from intended design with a complete statistical approach and high-fidelity simulations. A feasible strategy is to search for a robust turbine, that allows one to maintain high performance levels even when operating conditions depart from the original design intent, hence evaluating the benefit of the single uncertainty effect.

Such factors have an impact on turbine behavior in terms of velocity triangles and main aerodynamic boundary conditions, like pressure and temperature distributions. When analyzed in the design phase these effects can be well represented through variations of incidence, Reynolds number, pressure ratio, turbulence, fluid and roughness parameters:

- Velocity triangle variation has a direct impact on airfoil incidences, which strongly impacts on performance.
- Reynolds number and fluid/geometry parameters affect boundary layer transition and separation phenomena with a significant impact on profile losses.
- Pressure ratio variations can occur for different causes, e.g. airfoil blockage, leakages and cooling flows.

WORK DESCRIPTION

First of all, a suitable LPT baseline configuration obtained following standard design methodologies was chosen. This configuration is a 6-stage module, representative of a typical low pressure turbine for modern aircraft engines. It is the result of a three-year-long national research program conducted by Avio. The design process and the tools used to obtain this configuration are the same used, and later briefly described, in this work. The design was performed with optimization objectives on performance, weight, acoustic emissions, airfoil count and mechanical verification, and it differs from the one reported in this paper in that the robustness was not an objective function.

TABLE 1: LPT thermodynamic cycle data.

		TAKE OFF	CRUISE	APPROACH
T_0	K	1280	1000	980
p_0	kPa	723.1	229.7	346.4
α_{in}	deg	15	15	15
N	rpm	2437	2131	1711
$\dot{m}_{in}$	kg/s	141.3	52.2	79.5
PR	-	4.8	5.8	3.3
$\Delta H/T$	J/kg/K	377	355	274
u_{max}	m/s	-	211	-
α_{out}	deg	25	25	25

TABLE 2: LPT Geometrical boundary conditions.

Inlet Inner Radius	m	0.587
Inlet Outer Radius	m	0.687
Outlet Inner Radius	m	0.607
Outlet Outer Radius	m	0.946
Max Length	m	0.771

Baseline cross-section, thermodynamic cycle data at Approach, Cruise and Take-off conditions and geometrical boundary constraints are reported in Fig. 1 and in Tab. 1 and 2, respectively.

A CFD sensitivity analysis, based on the previously reported three main effects of variations due to model-to-reality differences, has shown that the most important influence on profile losses is related to the impact that such uncertainties have on local velocity triangles. These phenomena are mainly reflected as variations of incidence.

A design practice to verify if a row is robust with respect to incidence variations requires an evaluation of its performance under positive incidences of 5° and 10°, and then to verify that loss increases remain below $\Delta\zeta_{\text{Limit}}$ values of 1% and 3% respectively. This empiric criterion, frequently adopted by designers, has been chosen as the basis of the described work. The average incidence variations for the LPT module can be obtained by reducing the rotational speed by about 10% and 20% with respect to the design point.

$$\begin{aligned} \Delta\zeta_{\text{Limit @ }+5^\circ} &= (\zeta_{\text{Row @ }+5^\circ} - \zeta_{\text{Row @ DP}})_{\text{Limit}} &&= 1\% \\ \Delta\zeta_{\text{Limit @ }+10^\circ} &= (\zeta_{\text{Row @ }+10^\circ} - \zeta_{\text{Row @ DP}})_{\text{Limit}} &&= 3\% \end{aligned} \quad (1)$$

As reported in Fig. 2 (a), the interpolation of $\Delta\zeta_{\text{Limit}}$ values defines a critical line separating regions of robust and non-robust design.

This line is considered an essential reference for robustness assessment; for each turbine row it is possible to obtain a sensitivity curve to incidence variation that can be compared with the limit curve. If the analyzed row losses fall under the critical line, the blade is traditionally considered robust, showing that loss variations under positive incidence angles are lower than the limit value. On the contrary, if the row curve stays above the limit line, the row will be considered not robust. Negative incidences are usually not verified with this procedure because under such conditions the reduction of deflection more than compensates for the small loss increase linked to the non-optimal impact of the flow on the suction side of the profile leading to overall loss reductions.

For the purpose of this work, the robustness index needs to be mathematically defined and this can be done with the following approach: it is set to be null for a row performing exactly like the limit curve and to assume a value of one in the ideal case of a row exactly maintaining a

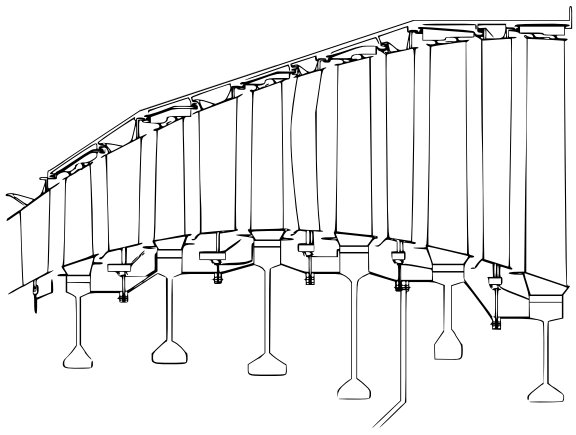

Figure 1: Baseline cross-section.

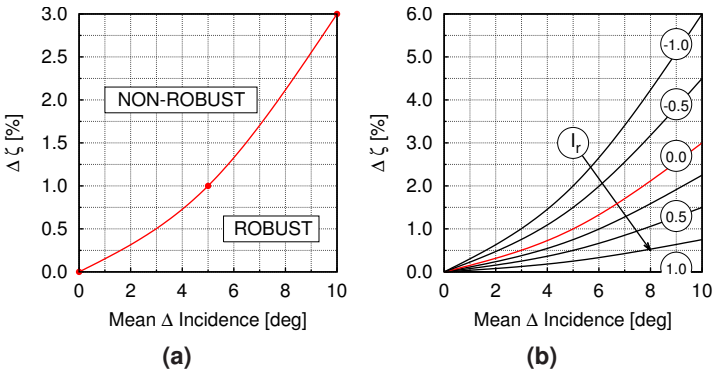

Figure 2: Robustness index definition.

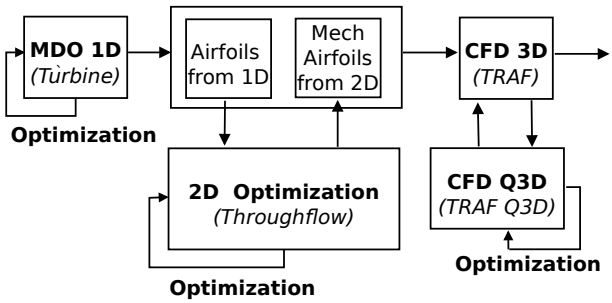

Figure 3: Design process flow chart.

flat performance profile. Using these two extreme values, the robustness index (Fig. 2 (b)) is defined in order to assume consistent decreasing values approaching the critical curve:

$$I_r = 1 - \frac{1}{2}\left[\left(\frac{\Delta\zeta_{\text{Row}}}{\Delta\zeta_{\text{Limit}}}\right)_{@\ +5^\circ} + \left(\frac{\Delta\zeta_{\text{Row}}}{\Delta\zeta_{\text{Limit}}}\right)_{@\ +10^\circ}\right] \tag{2}$$

where for each analyzed row, $\Delta\zeta_{Row}$ is defined as follows both for +5° and +10° incidence variations:

$$\begin{aligned}\Delta\zeta_{\text{Row @ }+5^\circ} &= \zeta_{\text{Row @ }+5^\circ} - \zeta_{\text{Row @ DP}} \\ \Delta\zeta_{\text{Row @ }+10^\circ} &= \zeta_{\text{Row @ }+10^\circ} - \zeta_{\text{Row @ DP}}\end{aligned} \tag{3}$$

The objective of the reported study is to increase the average value of row robustness indices during each optimization carried out within the design process (1D, 2D, Airfoil Optimization), as reported in Fig. 3.

The main phases in the design process are described below:

1D meanline analysis. A reduced number of basic input data, mainly describing the thermodynamic cycle, the geometrical boundary condition, the flow path and the corner points definition, the work split and reactions details and the airfoil count for each row defines a turbine module in a parametric manner. Thanks to a proprietary tool it is possible to aerodynamically analyze this configuration at meanline by solving Euler equations coupled with turbine losses correlations, i.e. C&C [13] or AMDCKO [14–16]. Fast calculations are carried out with a preliminary LPT cross section definition after mechanical verifications for turbine component geometries (containment for casing, vane and blade static

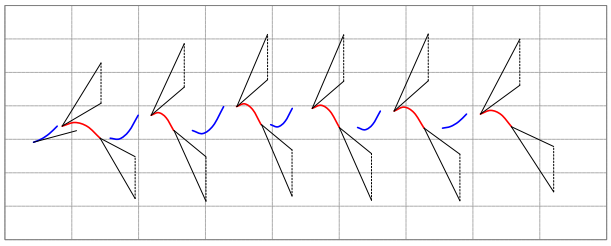

Figure 4: Velocity triangles at midspan (baseline configuration).

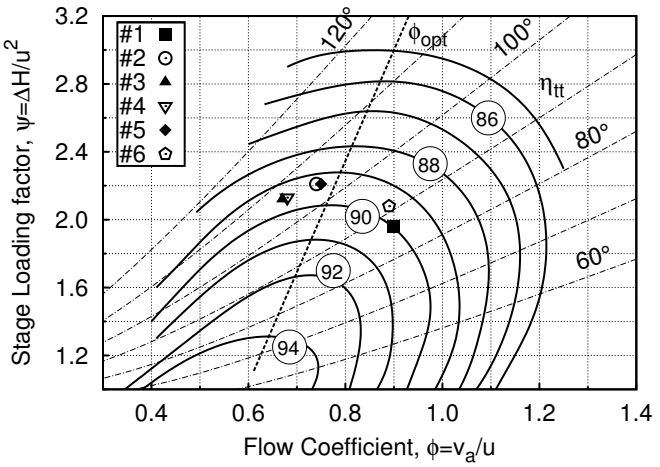

Figure 5: Smith diagram for baseline configuration.

TABLE 3: Main parameters for baseline configuration.

Row	*Zw*	*MR*	Reaction	*FT*	*AR*	*PR*
b1	1.04	1.37	0.37	93.5	3.4	1.16
v2	0.99	1.89		94.1	3.2	1.22
b2	0.98	1.68	0.42	107.1	4.1	1.20
v3	0.95	1.89		105.8	3.6	1.22
b3	0.83	1.83	0.45	107.8	4.7	1.21
v4	1.11	2.01		104.6	7.2	1.24
b4	0.97	1.94	0.46	105.4	5.2	1.24
v5	0.98	2.04		104.5	7.4	1.29
b5	0.99	1.80	0.43	104.2	5.7	1.28
v6	0.98	1.93		97.8	8.3	1.33
b6	1.06	1.61	0.39	93.0	6.3	1.29

analyses, disk burst, clashing, arms and jointed bolts), weight assessment and acoustic preliminary estimation. Specific custom objectives, such as robustness correlations in this study, could also be added and optimized thanks to a specific tool based on OLH sampling.

Figure 1 reports an example of a cross-section: the level of detail achievable in concept design phase is already evident. Figures 4-5 and Tab. 3 show other outputs for velocity triangles, a Smith diagram, and main design parameters.

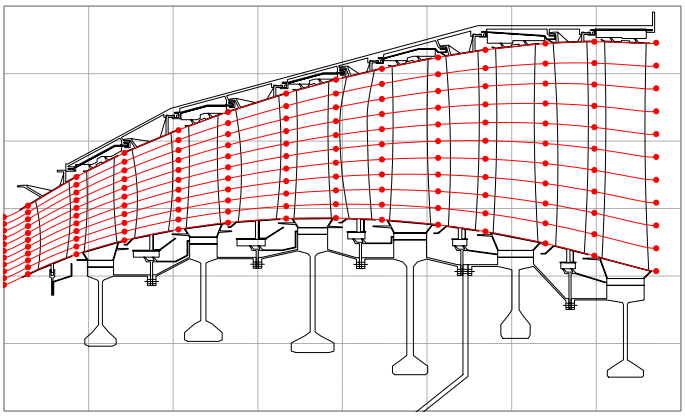

Figure 6: Streamline definition for through-flow analysis.

Parametric airfoil generator. Blade shape is built by means of a discrete number of spanwise sections, each defined in terms of 13 independent geometrical parameters. A 3D definition of each row for the LPT can be automatically generated using data from 1D meanline or 2D through-flow solutions by obtaining preliminary definition for parameters still not univocally defined from an industrial database. Such a parametric description of the profile is well-suited for implementation in an automatic optimization procedure as later reported in the airfoil study.

Through-flow analysis. This part of the design is aimed at optimizing the preliminary choice of spanwise work while the main 1D values remain unchanged. Main airfoil data at various sections for each row of the module can be used to set up a through-flow computation (SC90T code by PCA Eng.). A similar approach to the one used for meanline analyses is adopted on various streamlines as shown in Fig. 6 and similar correlations are implemented in the code with a more accurate evaluation of profile, secondary, clearance and windage losses.

CFD analyses. The computational framework is based on the TRAF code (Arnone [17]), a Q3D/3D multi-row, multi-block CFD solver for the RANS/URANS equations written in conservative form in a curvilinear, body-fitted coordinate system. The space discretization is based on a cell-centered finite volume scheme. Both scalar and matrix artificial dissipation models are available in the code. A dual-time- stepping method [18, 19] is used to perform time accurate calculations. The code features several turbulence closures, namely the algebraic Baldwin-Lomax model [20], the one-equation Spalart-Allmaras model [21], and the two-equation $k-\omega$ models (Wilcox's low/high Reynolds versions [22], and Menter's SST model [23]). A three-equation, transition-sensitive, turbulence model, based on the coupling of an additional transport equation for the so-called laminar kinetic energy (LKE) with the Wilcox's $k-\omega$ model is available for transitional, separated-flow configurations [24, 25]. The real gas behavior can be accounted for with a model based on the use of gas property tables generated off-line [26].

All the results presented in this work were obtained using 3D meshes of about 10^6 cells per row and the $k-\omega$ turbulence model (low Reynolds version). The mesh size was selected as a compromise between grid resolution, grid independence, and computational time. The Q3D version of the code was used in a multi-objective environment for the airfoil optimization.

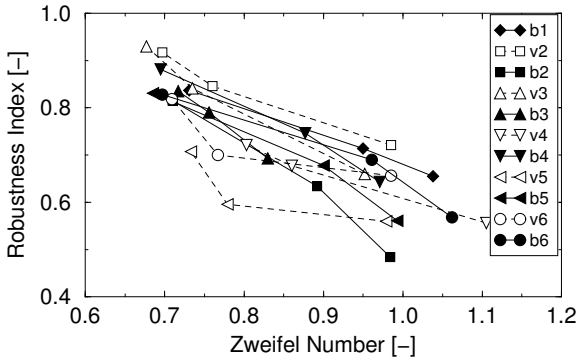

Figure 7: Robustness index vs. Zweifel number for each row.

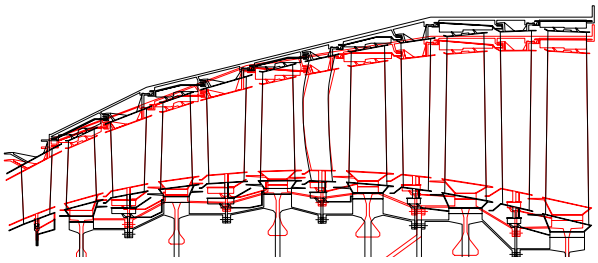

Figure 8: Cross section variation for aspect ratio sensitivity.

ROBUSTNESS OPTIMIZATION

1D study with CFD assessment. Starting from baseline design, an extended sensitivity analysis was performed to identify main 1D module parameters affecting robustness. In particular, new configurations were studied by modifying blade counts, work split stage distribution (Flow Turnings), Mach ratios and aspect ratios.

Figure 7 shows the results obtained from multistage CFD computations, in terms of robustness index from the analyses in which blade count was changed. The first vane is not included because its behaviour is not directly linked with RPM variation. The Zweifel parameter [27] has been chosen to represent the effect of solidity variations on the robustness index.

It is quite evident that a reduction in the Zweifel number is related to an increase in robustness. From this, one of the first options considered, in order to improve robustness, could be an increase of blade count that leads to lower Zweifel numbers. This possibility has to be avoided when possible because it completely disagrees with current design trends that are aimed at reducing weight and costs and thus tend towards a blade number limitation.

Another sensitivity analysis was performed changing the flow path height (Fig. 8), in particular, the cross section area was uniformly reduced by about 25%, while keeping the radius of the mean line unaltered. Accordingly, the mass flow rate was reduced in order to keep the Smith diagram of Fig. 5 unchanged. From this analysis, the effect on the aspect ratio is clear: last rows are, in fact, characterized by higher values of robustness index (Fig. 9) and this could be due to the reduced impact of secondary flow development on row performance. The effect is also evident looking at single values for each row, which increase with the aspect ratio. Figure 10 reports the robustness index trend with respect

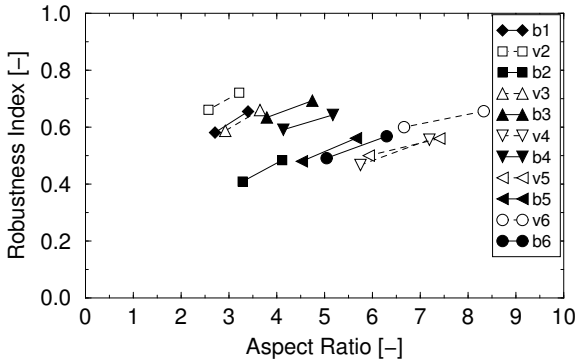

Figure 9: Robustness index vs. aspect ratio *AR* for each row.

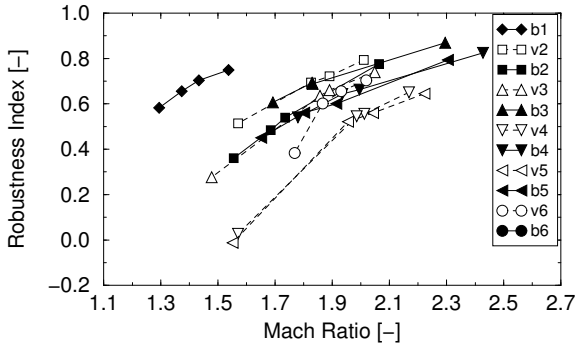

Figure 10: Robustness index vs. Mach ratio *MR* for each row.

to the ratio of outlet over inlet Mach numbers, representative of the acceleration of the flow on the profiles. It is evident that increasing *MR* brings an improvement of robustness index.

When analyzing vanes and blade curves, it is also possible to notice that the loading level on profiles, identified with flow turning, has a significant effect on robustness index. Central stages (e.g. stages #4 and #5) are more loaded, and are less robust than external stages (e.g. stages #1 and #2) which are unloaded.

All these data obtained from CFD numerical calculations have then been analyses using statistical methods, trying to define a correlation for robustness index respect to those parameters that more significantly affect it. A regression has been found with Zweifel number, flow turning, Mach ratio and aspect ratio as main parameters able to explain more than 80% of the robustness index variation:

$$I_r = -a_{Zw}Zw + a_{AR}AR + a_{FT}FT - a_{FT,2}FT^2 + a_{MR}MR - a_{MR,2}MR^2 - a_0 \quad (4)$$

a coefficients are intended to be positive. Two different functions were defined for vanes and blades to take into account effects due to different geometrical characteristics.

The correlation was then used to increase average row robustness with the 1D mean-line optimization tool and the obtained solution was verified by multistage CFD. Nevertheless, since this procedure was aimed at increasing the average value, robustness index can slightly decrease locally (as in Vane #2, Blade #4). Detailed results of robustness improvements for each row with respect to baseline (in brackets) are reported in Fig. 11.

2D study with CFD assessment. A similar approach has been used in the through-flow 2D design revision where mainly only the spanwise flow angle distribution is optimized, keeping the average value and all other main parameters in line with the previous 1D phase result. A DOE approach was used for the sensitivity analysis. Each spanwise distribution was changed, with respect to the original one, in a way to vary the outlet angle at specific spanwise locations, with linear or parabolic laws (see Fig. 12). Each analyzed configuration was defined to maintain average values

Thanks to regressions from the sensitivity analyses three robustness index functions, similar to the one presented in Eq. 4, were defined for three different spanwise sections to locally keep track of the impact of secondary flows and clearances.

The regressions were inserted in the through-flow optimization code in order to increase not only performance (as for standard baseline approach) but also the average robustness index. The obtained solution

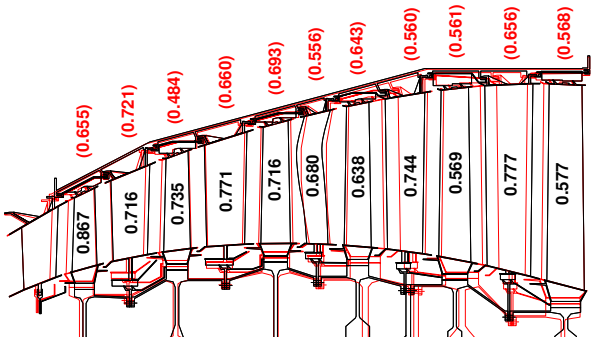

Figure 11: 1D robust configuration vs. baseline (red).

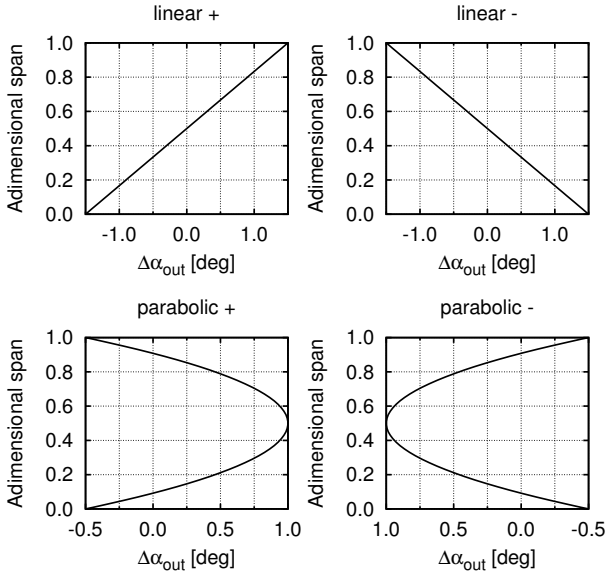

Figure 12: 2D Spanwise DOE for exit flow angles.

		Baseline	Final
R	Radius at LE	0.801	0.801
c_x	Axial Chord	0.034	0.034
c_t	**Tangential Chord**	0.0242	0.0209
UT	**Unguided Turning**	13.79	15.83
β_{in}	**Inlet Blade Ang.**	42.38°	47.06°
ε_{in}	**Inlet Wedge Ang.**	9.87°	8.05°
R_{LE}	**LE Radius**	0.0018	0.0019
β_{out}	**Exit Blade Ang.**	-68.15°	-68.99°
R_{TE}	TE Radius	0.0003	0.0003
N_b	N of blades	160	160
o	**Throat**	0.0133	0.0133
a_{LE}	**LE eccentricity**	0.0071	0.0074
a_{TE}	TE eccentricity	0.0003	0.0003

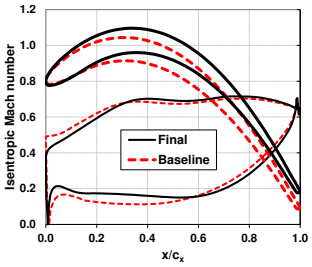

	Objective Function Value	
	Baseline	Final
$\eta@DP$	96.57%	96.69%
I_r	0.600	0.759
Ob($\dot{m}$)	100%	100%
Ob(Area)	100%	99.98%
Ob(Mach)	99.46%	99.27%
Ob(Shape)	99.99%	99.99%

Figure 13: Q3D optimization of each parametric section.

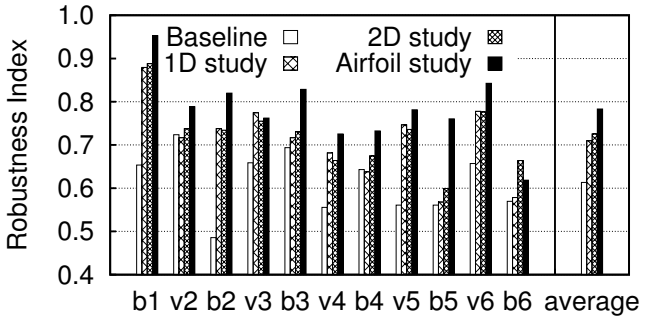

Figure 14: Robustness index during optimization phases.

was finally analyzed by 3D multistage CFD computation confirming TF results. The average robustness index improved from a baseline value of 0.614 to a 1D optimized value of 0.709 and then to a TF optimized value of 0.723.

Airfoil study. The third optimization step is dedicated to airfoil 3D revision to further improve the quality already achieved. This phase was accomplished by using an automatic procedure based on Q3D-CFD analyses on three streamline sections, hub (5% spanwise), mid and tip (95% spanwise). Profile parameterization is reported in Fig. 13, with, in bold, free parameters for this optimization phase.

The abovementioned procedure maximizes a multi-objective function opportunely weighted on the following goals: aerodynamic efficiency level, robustness index, 2D mass flow rate, maximum Mach number on the suction side (in order to contain excessive flow accelerations

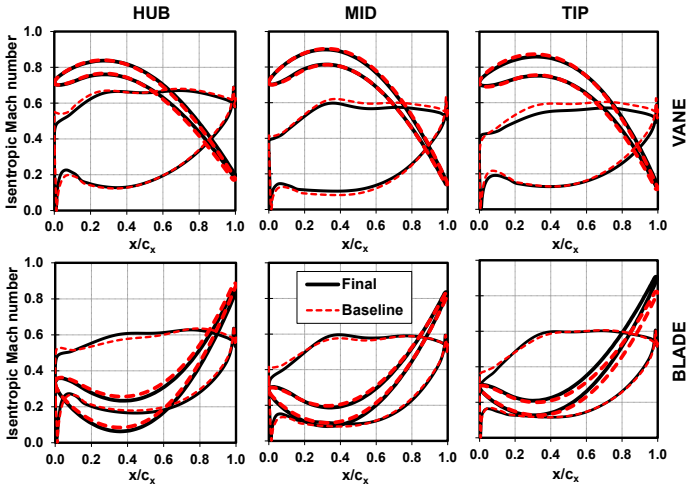

Figure 15: Isentropic Mach distributions for Stage #3 (baseline vs. final configuration).

on the blade), blade section area (with downward limitations needed for mechanical requirements) and a specific parameter to control shapes (in order to avoid convergence toward unacceptable geometries).

The values of these factors first and after the optimization phase are also reported in Fig. 13 (for blade #5 at midspan).

In order to evaluate the robustness index, all the tested geometries were analyzed not only at DP incidence, but also at +5° and +10°. Starting from optimization results, new 3D row geometry is then obtained by spanwise parabolic interpolation of each profile parameter.

Complete module CFD simulations are carried out in order to confirm improvements on performance at DP and on/off-design conditions. Figure 14 shows final values of the robustness index for each row compared with previous phases data; in this figure there is also the average value. The robustness improvement achieved by the final configuration and the advantages obtained in each optimization step are evident.

A statistical regression analysis was performed to highlight which geometrical airfoil parameters affect the robust design. In particular it has been found that the robustness is improved when the inlet metal angle is increased, thus reducing the design incidence. A smaller stagger angle is suggested together with higher values of unguided turning and a slightly lower value of the inlet wedge angle. In general, the aerodynamic load near the leading edge is reduced, the accelerating part is extended and a more aft-loaded airfoil is obtained. As can be expected, robust airfoils feature a thicker leading edge and an increased t_{max}/c value.

ROBUST DESIGN ADVANTAGES

The main parameters found to have a big impact in our studies are presented in Tab. 4, divided into the relative phase where they are addressed. The arrows show how they have to be moved with respect to standard design to improve robustness.

A comparison of isentropic Mach distributions, between the original baseline (red) and the final configuration (black), is already reported in Fig. 13 for midspan section of blade #5 and it is proposed in Fig. 15 for hub/mid/tip of stage #3. From these examples, it is possible to un-

TABLE 4: Main parameters impacting on robustness.

1D/2D study	Airfoil study
$MR \uparrow$	$Inc \downarrow$
$Zw \downarrow$	$UT \uparrow$
$AR \uparrow$	Stagger $\downarrow$
$FT \downarrow$	$t_{max}/c \uparrow$
	$t_{LE}/c \uparrow$
	$\varepsilon_{in} \downarrow$

TABLE 5: Main parameters for final configuration.

Row	*Zw*	*MR*	Reaction	*FT*	*AR*	*PR*
b1	0.82	1.76	0.63	84.8	4.2	1.20
v2	0.96	1.59		102.9	3.0	1.19
b2	0.78	1.81	0.51	102.3	5.0	1.19
v3	0.95	1.85		104.9	3.4	1.20
b3	0.86	1.94	0.48	105.1	5.6	1.21
v4	1.06	2.00		105.8	7.0	1.23
b4	0.84	1.94	0.46	105.3	7.3	1.24
v5	0.95	2.05		105.0	5.3	1.29
b5	0.84	1.84	0.44	105.5	7.3	1.30
v6	0.93	1.97		101.6	5.2	1.37
b6	0.93	1.49	0.33	96.8	7.3	1.29

derline the variation of parameters as reported in Tab. 4.

Row main parameters for the final robust optimized configuration are reported in Tab. 5. Comparing these values with the baseline configuration ones (see Tab. 3) it can be noticed that average *Zw* is reduced, average *MR* is increased, and is now more uniform between the rows, and reaction values as well as the average *AR* are generally increased.

Figure 16 shows a comparison among the baseline and the optimized configurations in terms of LPT efficiency as a function of rotational speed. For each configuration, five 3D CFD analyses have been performed, obtaining efficiencies at different operational RPM. The better performance at low rotational speeds denotes the fact that the robustness index of the final configuration has been appreciably increased. The efficiency gain of the final configuration with respect to the baseline is shown in Fig. 17.

It's interesting to notice that the final configuration presents a small performance benefit at nominal rotational speed. This appears to be in contrast with the fact that this configuration was obtained with a similar design process to the one used for the baseline configuration, but with an additional objective function based on robustness. The explanation could be that 1D, 2D and also Q3D optimization phases optimize each blade using simplified analyses, assuming that it works under specific inlet/outlet conditions that will differ slightly from the ones found in the 3D multistage CFD assessment. In this context the robust designed configuration can offer some advantages since it is less influenced by these uncertainties.

As can be noticed, a remarkable performance improvement can be achieved with the robust configuration at lower RPM. On the contrary, at higher rotational speeds, representative of negative incidence angles, the efficiency of the final configuration slightly decreases. This effect will be taken into account for the final assessment of the benefit stemming from the robustness optimization. However, the efficiency reduction at higher rotational speeds is not of major concern, since the model-to-reality discrepancies usually lead towards an increase in the average row incidence. This curve, in form of an explicit function, is implemented as surrogate emulator for a Monte Carlo analysis.

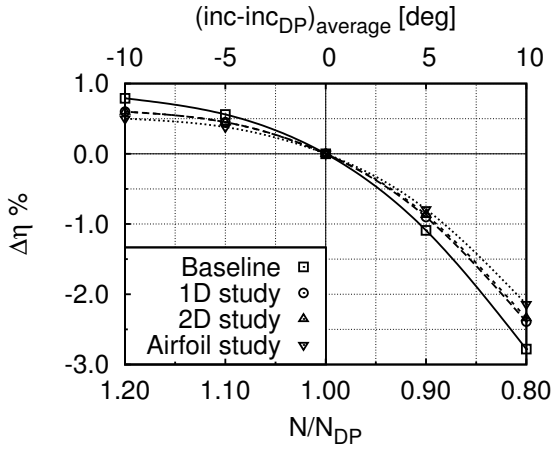

Figure 16: Efficiency at different rotational speeds.

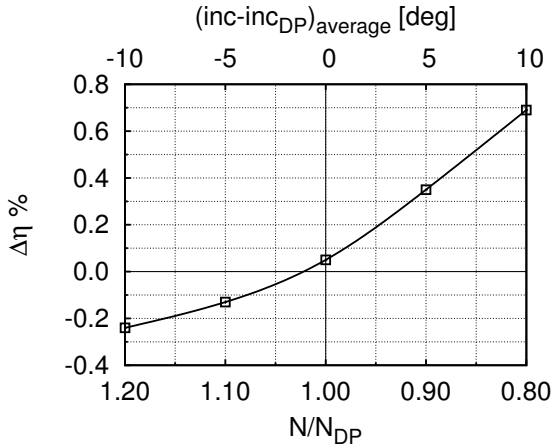

Figure 17: Final configuration efficiency gain.

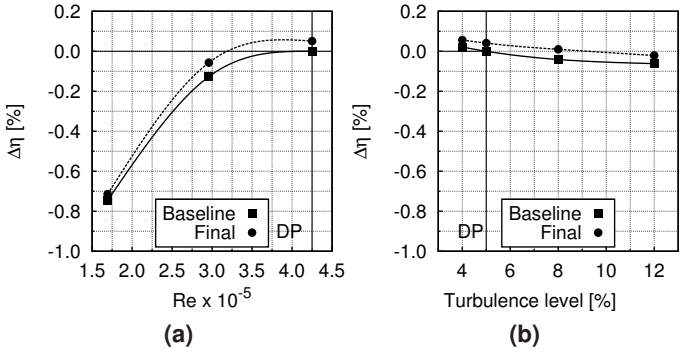

Figure 18: Reynolds and turbulence level effects.

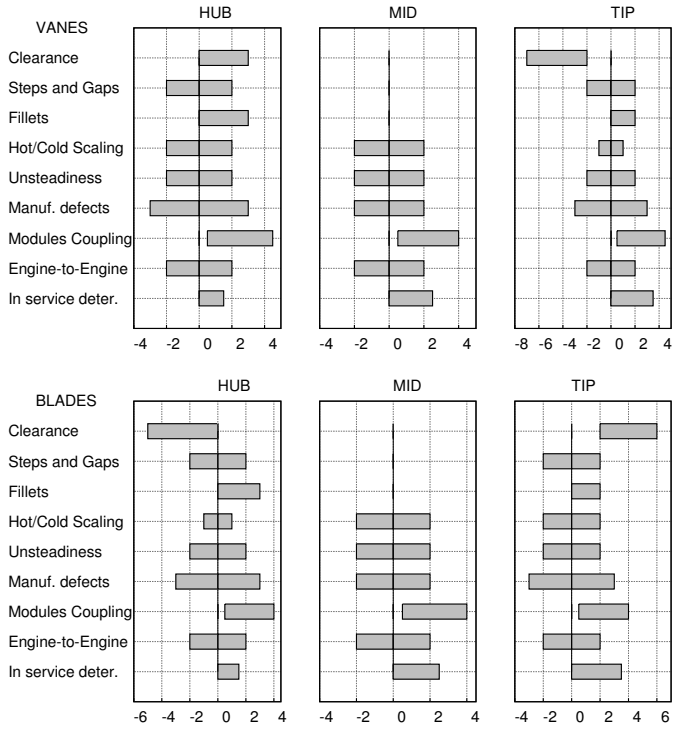

Figure 19: Range on incidence angle deviations due to some real vs. model variations.

TABLE 6: LPT thermodynamic cycle data.

		NEW	$^2/_3$ DET.	FULLY DET.
T_0	K	1000	1051	1073
p_0	kPa	229.73	224.83	222.25
N	rpm	2131	2125	2121
$\dot{m}_{\text{in}}$	kg/s	52.2	49.8	48.7

A comparison between baseline and improved configurations was carried out as a function of Reynolds number and turbulence level, and is reported in Fig. 18. It is interesting to notice that, even if the uncertainties on these parameters have not been included in the optimization of the module, the CFD analyses show that the robust configuration maintains better performance even when these conditions are changed. Further work to investigate these effects during the optimization phase to check if better improvements could be reached is foreseen.

From past, detailed numerical analyses, experimental and manufacturing data, and general experience on physical phenomena, the impact of model-to-reality discrepancies on vane and blade incidences was estimated and their ranges are briefly reported in Fig. 19, for mid-section as well as for hub and tip zones (first and last 10% of the span respectively). The data were obtained from different engines and rows. For example, the inclusion of blade fillets in the numerical model showed an overturning at the row exit near the endwalls, especially at the hub, where throats are narrower. Numerical simulations of endwall steps and gaps details have shown variations of $\pm 1^\circ$ on the exit flow angle.

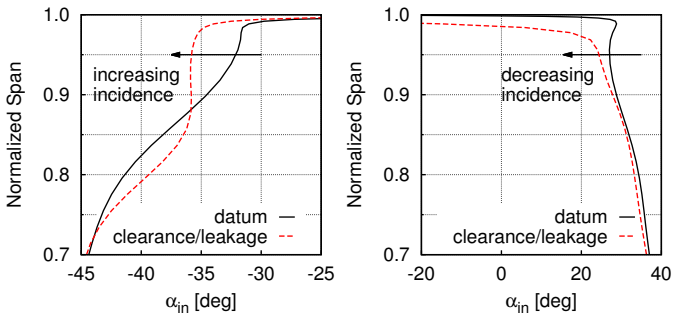

Figure 20: Effect of clearances and leakages on two adjacent rows (RTC tip zone).

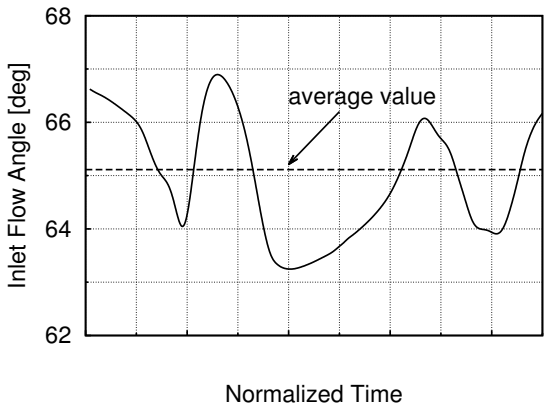

Figure 21: Steady vs. unsteady inlet flow angle.

Table 6 shows the impact of engine aging on the main design thermodynamic parameters, comparing the cycle data of a new engine with a $^2/_3$ and a fully deteriorated engine. A deterioration of the engine leads the inlet temperature for a LPT module to greatly increase and it brings a reduction of the corrected speed $N/\sqrt{T_0}$ of about 4% (corresponding to 2.5° incidence increase on the average).

The presence of rotor tip clearance and/or inter-stage seal cavities causes local incidence variations near the endwalls. In particular, the incidence is increased where the by-pass flow exits from the flow path and it is decreased where the flow re-enters in the main channel. Such an effect is shown in Fig. 20.

Figure 21 shows the time variation of the inlet flow angle at a fixed position in front of the blade leading edge compared with its average value. Only a fraction of the time period has been plotted for clarity, hence the angle is not periodic with the time span plotted. The presence of the wake changes the row incidence of about $\pm 2^\circ$ during a time period.

A Monte Carlo analysis has been conducted using the incidence variations reported in Fig. 19 and efficiency gains reported in Fig. 17. A flat probability distribution was assumed in the proposed ranges. Different simulations have been conducted for a new engine, a fully de-

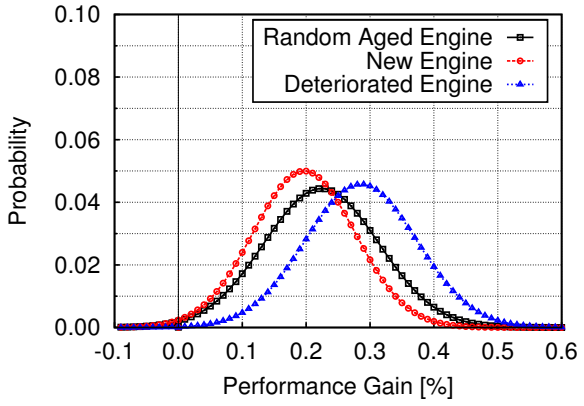

Figure 22: Performance benefit of optimized configuration.

teriorated engine and for a "random aged engine" during its flight life, including in different ways the effect of engine deterioration. Finally the results in terms of performance benefit are reported in Fig. 22.

From these results, the average LPT performance (the one obtained for a "random aged engine") benefit is 0.23% (for a new engine 0.20% and 0.28% for a fully deteriorated engine) corresponding to a fuel saving of roughly 0.20% for airline companies.

CONCLUSIONS

This paper reports the work of optimization on a LPT module aimed at increasing its robustness. The approach followed is described for each of the main phases of the design framework where it was applied.

The proposed methodology as well as the most important defined parameters have a general validity, and a similar method can be used on other engines and different components, too. However, more detailed work and analyses performed on different modules will be needed to derive more general rules (e.g. for the equation representing the robustness index as a function of main project parameters) and to better validate the output of this research. This could allow researchers to verify the increased importance of robustness optimization for new generation engines.

Finally a Monte Carlo simulation was performed to estimate the attainable advantages in terms of performance, showing non-negligible advantages for airlines in terms of SFC. It should be noted that the values adopted for the incidence angle variations caused by model-to-reality deviations will need further assessment, and internal as well as European-Union-funded research projects are already planned in order to validate those ranges and extend their generality.

This work has shown that going over the historically used criteria to verify profile robustness using a revised design process to take into account robustness during the optimization phases offers remarkable performance advantages. It will also be interesting to carry out a multidisciplinary research project to verify the impact of this study on parameters such as the module weight and the airfoil count, and to investigate the possibility of optimizing such effects.

ACKNOWLEDGMENTS

The authors would like to thank Prof. Andrea Arnone and Mr. Ennio Spano for the important contributes given and the supervision work. Special acknowledgments go to involved aero-teams.

NOMENCLATURE

a	Robustness correlation coefficient
AR	Aspect Ratio
c	Airfoil chord
FT	Flow Turning
I_r	Robustness index
Inc	Incidence
M	Mach number
MR	Mach Ratio, $MR = M_{out}/M_{in}$
N	Rotational speed [rpm]
p_0	Inlet total pressure
PR	Total-to-total pressure ratio
t	Airfoil thickness
T_0	Inlet total temperature
u	Peripheral speed
UT	Unguided Turning
Zw	Zweifel number

Greek

α	Swirl angle
$\Delta\zeta_{\text{Limit}}$	Maximum allowable losses variation
$\Delta\zeta_{\text{Row}}$	Row losses variation with respect to DP
ε	Wedge angle
η	Efficiency
ζ_{Row}	Row losses

Subscripts

in	Inlet
max	Maximum value
out	Outlet

Acronyms

ACARE	Advisory Council for Aeronautics Research in Europe
AMDCKO	Ainley-Mathieson-Dunham-Came-Kacker-Okapuu
BPR	By-Pass Ratio
C&C	Craig & Cox
CAE	Computer-Aided Engineering
CFD	Computational Fluid Dynamics
DOE	Design Of Experiments
DP	Design Point
FF	Flow Function
HL	High Lift
HPT	High Pressure Turbine
HSL	High Stage Loading
LE	Leading Edge
LPT	Low Pressure Turbine
MDO	Multi Disciplinary Optimization
OLH	Optimal Latin Hypercube
QFD	Quality Function Deployment
SFC	Specific Fuel Consumption
TCF	Turbine Center Frame
TF	Through-Flow

REFERENCES

[1] ACARE, 2001, "European Aeronautics: A Vision for 2020-Meeting Society's Needs and Winning Global Leadership". Advisory Council for Aeronautical Research in Europe, http://www.acare4europe.org.

[2] Garrison, L. and Walter, S., 2009, "Robustness Assessment of a Prediffuser, Strut and Frame". ASME paper GT2009-60163.

[3] Kumar, A., Nair, P. B., Keane, A. J., and Shahpar, S., 2008, "Robust Design Using Bayesian Monte Carlo". Int. Journal for Numerical Methods in Engineering, **73** (11), pp. 1497–1517.

[4] Kumar, A., Keane, A. J., Nair, P. B., and Shahpar, S., 2006, "Robust Design of Compressor Fan Blades Against Erosion". Journal of Mechanical Design, **128** (4), pp. 864–873.

[5] Ghisu, T., Parks, G. T., Jarret, J. P., and Clarkson, P. J., 2011, "Robust Design Optimization of Gas Turbine Compression Systems". AIAA Journal of Propulsion and Power, **27** (2), pp. 282–295.

[6] Karl, A., May, G., Barcock, C., Webster, G., and Bayley, N., 2006, "Robust Design – Methods and Applications to Real World Examples". ASME paper GT2006-90649.

[7] Wallace, J. M., Wojcik, S., and Mavris, D. N., 2003, "Robust Design Analysis of a Gas Turbine Component". ASME paper GT2003-38546.

[8] De Poli, P., Frola, G., Gallizio, M., Fattore, L., and Mattone, M., 2006, "Multi-disciplinary Integration and Robustness Evaluation Applied to Low Pressure Turbine Casing Design". ASME paper GT2006-90464.

[9] Chen, W. and Lewis, K., 1999, "A Robust Design Approach for Achieving Flexibility in Multidisciplinary Design". AIAA J., **37** (8), pp. 982–989.

[10] Egorov, I. N., Kretinin, G. V., and Leshchenko, I. A., 2002, "How to Execute Robust Design Optimization". AIAA paper 2002-4328.

[11] Panchenko, Y., Moustapha, H., Mah, S., Patel, K., Dowhan, M. J., and Hall, D., 2002, "Preliminary Multi-Disciplinary Optimization in Turbomachinery Design". RTO-MP-089.

[12] Denton, J., 2010, "Some Limitations of Turbomachinery CFD". ASME paper GT2010-22540.

[13] Craig, H. R. M. and Cox, H. J. A., 1970, "Performance Estimation of Axial Flow Turbines". Proc. Instn. Mech. Engrs., **185**, pp. 407–424.

[14] Ainley, D. G. and Mathieson, G. C. R., 1957, "A Method of Performance Estimation for Axial-Flow Turbines". Aeronautical Research Council R&M 2974.

[15] Dunham, J. and Came, P. M., 1970, "Improvements to the Ainley-Mathieson Method of Turbine Performance Prediction". Journal of Engineering for Power, **92** (3), pp. 252–256.

[16] Kacker, S. C. and Okapuu, U., 1982, "A Mean Line Prediction Method for Axial Flow Turbine Efficiency". Journal of Engineering for Power, **104**, pp. 111–119.

[17] Arnone, A., 1994, "Viscous Analysis of Three–Dimensional Rotor Flow Using a Multigrid Method". ASME J. Turbomach., **116** (3), pp. 435–445.

[18] Arnone, A. and Pacciani, R., 1996, "Rotor-Stator Interaction Analysis Using the Navier-Stokes Equations and a Multigrid Method". ASME J. Turbomach., **118** (4), pp. 679–689.

[19] Jameson, A., 1991, "Time Dependent Calculations Using Multigrid with Applications to Unsteady Flows Past Airfoils and Wings". AIAA paper 91–1596.

[20] Baldwin, B. S. and Lomax, H., 1978, "Thin Layer Approximation and Algebraic Model for Separated Turbulent Flows". AIAA paper 78–257.

[21] Spalart, P. R. and Allmaras, S. R., 1994, "A One–equation Turbulence Model for Aerodynamic Flows". La Recherche Aérospatiale, **1**, pp. 5–21.

[22] Wilcox, D. C., 1998, *Turbulence Modeling for CFD*, 2nd edition, DCW Ind. Inc., La Cañada, CA, USA, ISBN 1-928729-10-X.

[23] Menter, F. R., 1994, "Two–Equations Eddy Viscosity Turbulence Models for Engineering Applications". AIAA J., **32** (8), pp. 1598–1605.

[24] Pacciani, R., Marconcini, M., Fadai-Ghotbi, A., Lardeau, S., and Leschziner, M. A., 2011, "Calculation of High-Lift Cascades in Low Pressure Turbine Conditions Using a Three-Equation Model". ASME J. Turbomach., **133** (031016).

[25] Pacciani, R., Marconcini, M., Arnone, A., and Bertini, F., 2011, "An Assessment of the Laminar Kinetic Energy Concept for the Prediction of High-Lift, Low-Reynolds Number Cascade Flows". Proc. I.Mech.E. Part A: J. of Power and Energy, **225** (7), pp. 995–1003.

[26] Boncinelli, P., Rubechini, F., Arnone, A., Cecconi, M., and Cortese, C., 2004, "Real Gas Effects in Turbomachinery Flows: a CFD Model for Fast Computations". ASME J. Turbomach., **126** (2), pp. 268–276.

[27] Zweifel, O., 1954, "Die Frage der Optimalen Schaufelteilung Bei Beschaufelungen von Turbomaschinen, Insbesondere Bei Grosse Umlenkung in den Schaufelreihen". Brown Boveri und Co. BBC-Mitt, **32** (12), pp. 436–444.